Extent of Reduction of Vanadium Oxides during Catalytic Oxidation of Alkanes Measured by in-Situ UV−Visible Spectroscopy

Morris D. Argyle, Kaidong Chen,† Carlo Resini,‡ Catherine Krebs,§ Alexis T. Bell,* and Enrique Iglesia*

Chemical Sciences Division, E. O. Lawrence Berkeley National Laboratory, and Department of Chemical Engineering, University of California, Berkeley, California 94720-1462

Received: August 19, 2003; In Final Form: October 29, 2003

In-situ UV−visible spectroscopy was used to measure the extent of reduction of active centers in VO_x/γ-Al_2O_3 during oxidative dehydrogenation (ODH) of propane. Prevalent extents of reduction (0.062 to 0.30 e^-/V) are much smaller than required for the formation of stoichiometric V^{3+} or V^{4+} suboxides. Surface oxygen atoms are the most abundant reactive intermediates during propane ODH, as previously suggested by kinetic and isotopic studies. These measurements involved the rigorous calibration of UV−visible intensities in the pre-edge region using quantitative reoxidation of a small number of centers reduced in H_2. Transients observed during changes in C_3H_8 and O_2 concentrations indicate that only a fraction of the prevalent reduced centers (∼30−40%) are active in catalytic turnovers, while the rest are reoxidized in time scales much longer than turnover times. The number of catalytically relevant reduced centers depends only on C_3H_8/O_2 ratios, and not on individual reactant concentrations, indicating that oxygen vacancies are the predominant reduced centers and that hydroxyls and alkoxides are present at much lower concentrations. The fraction of V-atoms that exist as catalytically reduced centers and the rate of propane ODH (per exposed V-atom) increase with increasing vanadia surface density and domain size up to surface densities typical of polyvanadate monolayers (∼7.5 V/nm^2) and then reach nearly constant values at higher surface densities. This relation between the extent of reduction during catalysis and the propene formation rates confirms the redox nature of catalytic cycles and the exclusive kinetic relevance of the reduction part of the cycle, in which C−H bonds are activated using lattice oxygen atoms. This method for measuring the extent of reduction during catalysis using pre-edge features in the UV−visible spectrum provides greater sensitivity and time resolution than X-ray absorption and UV−visible spectroscopic methods based on near-edge spectral features. The approach and initial results seem generally applicable to oxidation reactions using lattice oxygens as reactive intermediates.

Introduction

Oxidative alkane dehydrogenation (ODH) on VO_x domains involves Mars-van Krevelen redox cycles using lattice oxygen and reduced V^{3+} or V^{4+} centers as reactive intermediates.[1−11] Mechanistic studies have shown that reduced centers are present at low concentrations during steady-state catalysis,[10,11] a conclusion specifically confirmed for *n*-butane oxidation on vanadyl-pyrophosphates (VPO) using in-situ X-ray absorption spectroscopy.[12] Our efforts to detect reduced centers in supported VO_x and MoO_x catalysts using near-edge X-ray absorption spectra during propane ODH did not succeed, because of the overlapping nature of near-edge features for various oxidation states of V and Mo absorbers and of the low concentration of reduced centers. These difficulties led us to seek simpler and more sensitive methods to measure the number of reduced centers on metal oxides during catalytic oxidation. We confronted similar sensitivity issues when using another technique of choice for assessing electronic structure and extent of reduction, involving measurements of near-edge absorption features in the UV−visible spectrum of oxide catalysts.

Diffuse reflectance UV−visible spectroscopy probes the electronic structure of oxide domains commonly used in alkane ODH catalysis.[6−9,13−16] Edge energies depend sensitively on domain size; they decrease with increasing domain size because charge is more effectively delocalized when larger domains are supported on insulating oxides.[10,11] Absorption edge energies in the UV−visible spectrum depend weakly on oxidation state, unless reduction processes significantly distort cation coordination symmetry;[13,17] thus, edge energies are unreliable as probes of the number and type of reduced centers prevalent during steady-state oxidation catalysis (e.g., vacancies, OH groups, alkoxides). Previous studies have estimated extents of reduction in metal oxides from measurements of near-edge spectral changes by using linear interpolations between spectra for stoichiometric oxides and for suboxides with stable structures formed by reduction in H_2.[17−28]

We report here a direct method for measuring the number of reduced centers during alkane oxidation catalysis on metal oxides. As described in a preliminary communication,[29] this method is based on measured changes in the pre-edge portion of UV−visible spectra. Its application is demonstrated here for the specific case of propane ODH on VO_x/Al_2O_3 catalysts, but the method is generally applicable to oxide catalysts and to catalytic oxidations requiring redox cycles. This technique

* Authors to whom correspondence should be addressed. E-mail: iglesia@cchem.berkeley.edu; bell@cchem.berkeley.edu.

† Current address: Chevron-Texaco Research and Technology Company, 100 Chevron Way, Richmond, CA 94802.

‡ Current address: University of Genoa, Ple. J. F. Kennedy, I-16129 Genoa, Italy.

§ Current address: Technical University of Hamburg-Harburg, 21071, Hamburg, Germany.

10.1021/jp030989m CCC: $27.50
Published on Web 01/27/2004

involves rigorous calibration of the number of reduced centers using a mild reduction in H_2, subsequent quantitative reoxidation, and the measurement of intensity in the pre-edge region during these treatments and during catalytic oxidation reactions.

Experimental Section

VO_x/Al_2O_3 catalysts were prepared by incipient wetness impregnation of γ-alumina (Degussa, A. G., 100 m^2/g) with aqueous solutions of ammonium metavanadate (99%, Aldrich, Inc.) and oxalic acid (Mallinckrodt A. G.) (1:2 by weight, pH ~2). The impregnated samples were dried, crushed, treated in dry air at 773 K, and ground into fine powders (45−100 μm) using a mortar and pestle. Catalyst synthesis procedures and structural characterization data were reported previously.[7−9] Three V_2O_5/γ-Al_2O_3 samples with 3.5, 10, and 30 wt % V_2O_5 and vanadia surface densities of 2.3, 8.0, and 34 V/nm^2, respectively, were used in this study.[7,8] Samples were treated at 773 K before each experiment in 5% O_2 (Airgas, 99.999%), in He (Airgas, 99.999%), or Ar (Airgas, 99.999%). Previous UV−visible and Raman spectroscopic studies showed that 3.5 wt % V_2O_5/Al_2O_3 (2.3 V/nm^2) contains predominantly isolated monovanadates,[8] 10 wt % V_2O_5/Al_2O_3 (8.0 V/nm^2) consists of polyvanadate domains coexisting with trace amounts of V_2O_5 crystallites, and 30 wt % V_2O_5/Al_2O_3 (34 V/nm^2) contains large V_2O_5 crystallites.[7]

UV−visible spectra were collected using a Cary 4 Varian spectrophotometer with a Harrick Scientific diffuse reflectance attachment (DRP-XXX) and a reaction chamber (DRA-2CR). The reaction cell was modified with a quartz frit to support samples and to improve flow uniformity. Two spectrophotometer modes were used to collect UV−visible spectra. One mode was used to measure conventional spectra in the 1.49−4.59 eV range (0.00186 eV steps, ~167 s per spectrum) during steady-state propane ODH. Spectra were initially referenced to MgO and ultimately referenced to the spectrum for each fresh catalyst in its highest oxidation state. Another operating mode was used to measure transient responses during propane ODH after abrupt changes in O_2 or C_3H_8 concentrations. In this mode, intensities were monitored at a single energy (1.86 eV) in the pre-edge region with a time resolution of 0.1−1 s.

Flow rates were kept at 1.67 $cm^3\ s^{-1}$ using mass flow controllers (Porter Instrument) for individual C_3H_8/Ar, O_2/Ar or O_2/He, and Ar streams in order to achieve the desired concentrations of each reactant. These flow rates corresponded to a space velocity of 50 $cm^3\ s^{-1}g^{-1}$ for the amounts of catalyst used in this study (~30 mg). Rapid switches between one reactant composition and another were made using an electrically-actuated four-way valve (Valco Instruments Company). The reaction temperature was held at 603 K and treatments in O_2-containing streams, intended to reoxidize samples, were carried out at similar or higher temperatures (up to 773 K). A thermocouple located within the catalyst bed was used to measure local temperatures; a thermocouple inserted within the heater beneath the sample holder recorded temperatures as much as 100 K above sample temperatures, as previously reported.[17,19] Propane ODH experiments were conducted at 603 K using C_3H_8 (Airgas, 99.9%) and O_2 (Airgas, 99.99%) reactants diluted to the desired partial pressures with Ar (Airgas, 99.999%). Partial pressures for each reactant were independently varied from 1.0 to 16 kPa, while keeping the other reactant at 4.0 or 8.0 kPa; the intervals between compositional changes were 300 s. In some experiments, water was added to $C_3H_8-O_2$ streams by flowing 1.0 kPa H_2 (Airgas, 99.99%) in Ar (Airgas, 99.999%) over CuO (Aldrich, 100 g, 13 wt % CuO/Al_2O_3) at 623 K to convert all H_2 to H_2O. All lines after this reactor were kept at 400 K to prevent condensation.

H_2 reduction measurements were carried out at 603 K using pure H_2 (Airgas, 99.99%) for 5, 10, 15, 20, or 30 min. The reactor was flushed with He (Airgas, 99.999%) for 180 s, while the sample was rapidly quenched to ambient temperature by removing the reactor from the furnace and flowing air past its external walls. An oxygen back-titration was conducted after each H_2 treatment using 5.0 kPa O_2 (Scott, 99.99%) in He during rapid heating from 298 to 773 K at 1.67 K s^{-1}. The O_2 concentration in the effluent was continuously monitored by mass spectrometry (Leybold-Inficon Transpector 2.0, 100 AMU). The resulting peak was integrated using Peakfit 4.0 (Jandel Scientific Software) to measure the amount of O_2 consumed during each oxidation (TPO).

The H_2 reduction and TPO data were used to obtain calibration curves relating UV−visible intensities in the pre-edge and edge regions to the number of reduced centers for each sample. Quantification of the reduced centers by direct reoxidation following ODH is not sufficiently accurate, because purging the reactants and quenching the reaction alters the extent of reduction prevalent during steady-state catalysis. A stoichiometric reductant (H_2) was therefore used to reduce fresh samples for controlled periods of time; this process was followed by measurements of the oxygen deficiency in each sample from the number of O_2 molecules required to recover the initial UV−visible spectrum during reoxidation in O_2/He. The number of electrons introduced during reduction and removed during oxidation was estimated by assuming that each O-atom causes a two-electron oxidation event.

Diffuse reflectance spectra were analyzed using Kubelka−Munk treatments.[30−32] The diffuse reflectance for infinitely thick samples (R_∞) is given by the reflectance of a sample of finite thickness (R_{sample}) divided by the reflectance of highly reflective standards ($R_{reference}$), such as MgO (the standard initially used here):

$$R_\infty = R_{sample}/R_{reference} \quad (1)$$

The Kubelka−Munk function, $F(R_\infty)$

$$F(R_\infty) = (1 - R_\infty)^2/2R_\infty = K/S \quad (2)$$

represents the ratio of absorption (K) and scattering (S) coefficients. Scattering coefficients depend weakly on photon energy, but absorption cross-sections increase abruptly as electronic transitions become possible with increasing incident photon energy. Thus, $F(R_\infty)$ provides a measure of absorbance throughout the experimental spectral range.[31] The reflectance relative to the fully oxidized sample ($R_{\infty,rel}$) was defined as

$$R_{\infty,rel} = (R_{reduced\ sample}/R_{MgO})/(R_{oxidized\ sample}/R_{MgO}) = R_{reduced\ sample}/R_{oxidized\ sample} \quad (3)$$

This reflectance was used instead of that relative to MgO because fully oxidized samples provided a relevant standard spectrum measured in close temporal proximity to the reduction experiments. Spectra for fully oxidized samples were obtained before each experiment and provided a reliable internal reference. This relative reflectance (eq 3) gave reproducible absorbance results.

Results and Discussion

Figures 1a and 1b show the time evolution and relative magnitude of the spectral features detected in the pre-edge and

edge regions for 10 wt % V_2O_5/Al_2O_3 (8.0 V/nm^2) and 3.5 wt % V_2O_5/Al_2O_3 (2.3 V/nm^2), respectively, during propane ODH at 603 K (14 kPa C_3H_8, 1.7 kPa O_2). The spectrum with the lowest absorbance in the pre-edge region ($<\sim$2 eV) in each figure corresponds to the fresh catalyst in its highest oxidation state and shows a band at $\sim$4.2 eV (33 000 cm^{-1}) corresponding to V^{5+}. The two spectra with the stronger pre-edge absorbances in each figure were measured 300 s and 2 h after starting catalytic ODH reactions. The pre-edge absorbance increased markedly with reaction time, mostly during the first 300 s after contact with $C_3H_8-O_2$ reactants; the intensity of the absorption edge features concurrently decreased with increasing reaction time. Pre-edge features at $\sim$1.8 eV (14 500 cm^{-1}) for 10 wt % V_2O_5/Al_2O_3 and $\sim$1.9 eV (15 500 cm^{-1}) for 3.5 wt % V_2O_5/Al_2O_3, arise from d−d transitions in reduced centers (V^{3+}/V^{4+}); these transitions become possible during reduction as electrons occupy d-orbitals normally empty in cations in their highest oxidation state.[17,25] An isosbestic point is located at 2.7 eV (21 800 cm^{-1}) for 10 wt % V_2O_5/Al_2O_3 and at 2.8 eV (23 000 cm^{-1}) for 3.5 wt % V_2O_5/Al_2O_3. Figure 1 shows that these d−d transitions appear in a spectral region devoid of background absorption for freshly oxidized samples; therefore, this approach provides much more accurate measurements than methods based on changes in the intensity of edge features in UV−visible and X-ray absorption spectra. UV−visible absorption features at the edge arise from O-to-V ligand-to-metal charge transitions (LMCT), which are less sensitive to d-orbital occupation than d−d transitions. The absorption edge decreases in intensity with decreasing average V oxidation state because ligand-to-metal charge transfer becomes more difficult for lower cation valences, for which the lowest unoccupied states are partially filled, thus requiring electron transfer to higher energy states.[33]

Although changes in the pre-edge and edge regions are similar in magnitude (Figure 1), relative changes are about 10 times greater for pre-edge than for edge features (Figure 2). Figures 2a and 2b show changes in relative absorbance (referenced to fully oxidized samples using eq 3) during H_2 reduction for 10 wt % V_2O_5/Al_2O_3 (8.0 V/nm^2) and for 3.5 wt % V_2O_5/Al_2O_3 (2.3 V/nm^2), respectively, at 300 s increments. Relative spectra were obtained by dividing the spectrum after each H_2 treatment period by the spectrum of the corresponding fully oxidized sample (eq 3) and converting the resulting relative reflectance into absorbance using the Kubelka−Munk function (eq 2). Both spectral regions contain equivalent information, but pre-edge features avoid some disadvantages of intensity measurements at the edge. Highly absorbing samples, with small values of R_∞, lead to large $F(R_\infty)$ values; thus, relative differences in regions of large $F(R_\infty)$, such as the edge region, become less sensitive to changes in extent of reduction than corresponding changes in the pre-edge region.

Figures 3a and 3b show the relative absorbance (normalized per V-atom) as a function of the extent of reduction, defined as the average number of electrons transferred per V-atom in the sample (e$^-$/V). The ordinate in these figures was determined by integrating changes in $F(R_{\infty,\mathrm{rel}})$ in either pre-edge (1.49−1.86 eV; Figure 3a) or edge (2.73−3.53 eV; Figure 3b) regions after H_2 reduction. The extent of reduction shown in the abscissa was measured from the amount of O_2 required to fully restore the spectrum to that of the fresh sample. The extents of reduction shown in the calibration curves in Figures 3a and 3b are similar to those measured during propane ODH (0−0.6 e$^-$/V) and smaller than those for stoichiometric vanadium suboxides. The data in Figure 3a are based on pre-edge spectral changes. The same linear relation between $F(R_{\infty,\mathrm{rel}})$ and e$^-$/V was obtained for all samples using pre-edge spectral changes (Figure 3a),

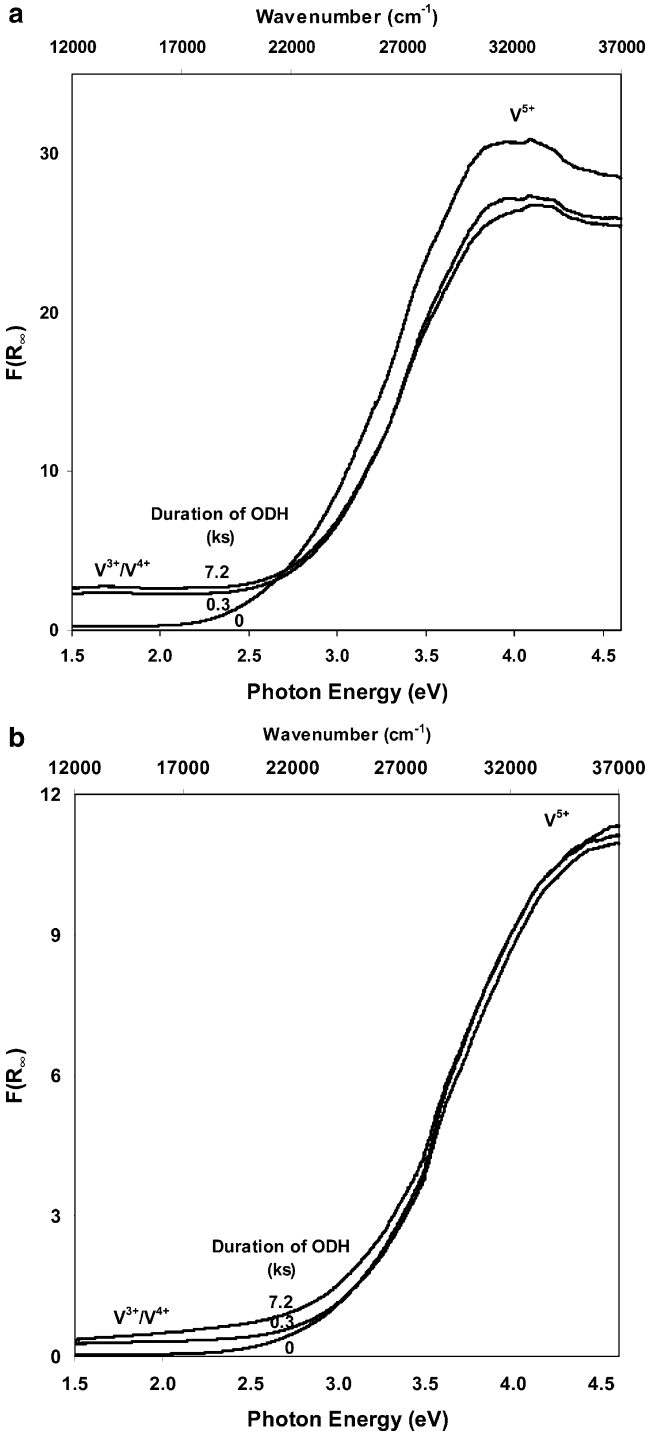

Figure 1. (a) UV−visible spectra of 10 wt % V_2O_5/Al_2O_3 (8.0 V/nm^2) before and during propane oxidative dehydrogenation, where the R_∞ reference is MgO [5 kPa O_2, balance Ar during oxidation; 14 kPa C_3H_8, 1.7 kPa O_2, balance Ar, 603 K]. (b) UV−visible spectra of 3.5 wt % V_2O_5/Al_2O_3 (2.3 V/nm^2) before and during propane oxidative dehydrogenation, where the R_∞ reference is MgO [5 kPa O_2, balance Ar during oxidation; 14 kPa C_3H_8, 1.7 kPa O_2, balance Ar, 603 K].

independent of V content. The edge features also lead to linear relations, which differ in slope, however, for samples with different V-content (Figure 3b).

The data in Figures 3a and 3b were used to determine extents of reduction during propane ODH at 603 K (14 kPa C_3H_8, 1.7 kPa O_2) from either pre-edge or edge spectral regions (Table 1). The overall extents of reduction measured from pre-edge and edge regions are similar for 3.5 wt % V_2O_5/Al_2O_3 (2.3 V/nm^2), indicating that pre-edge and edge regions provide

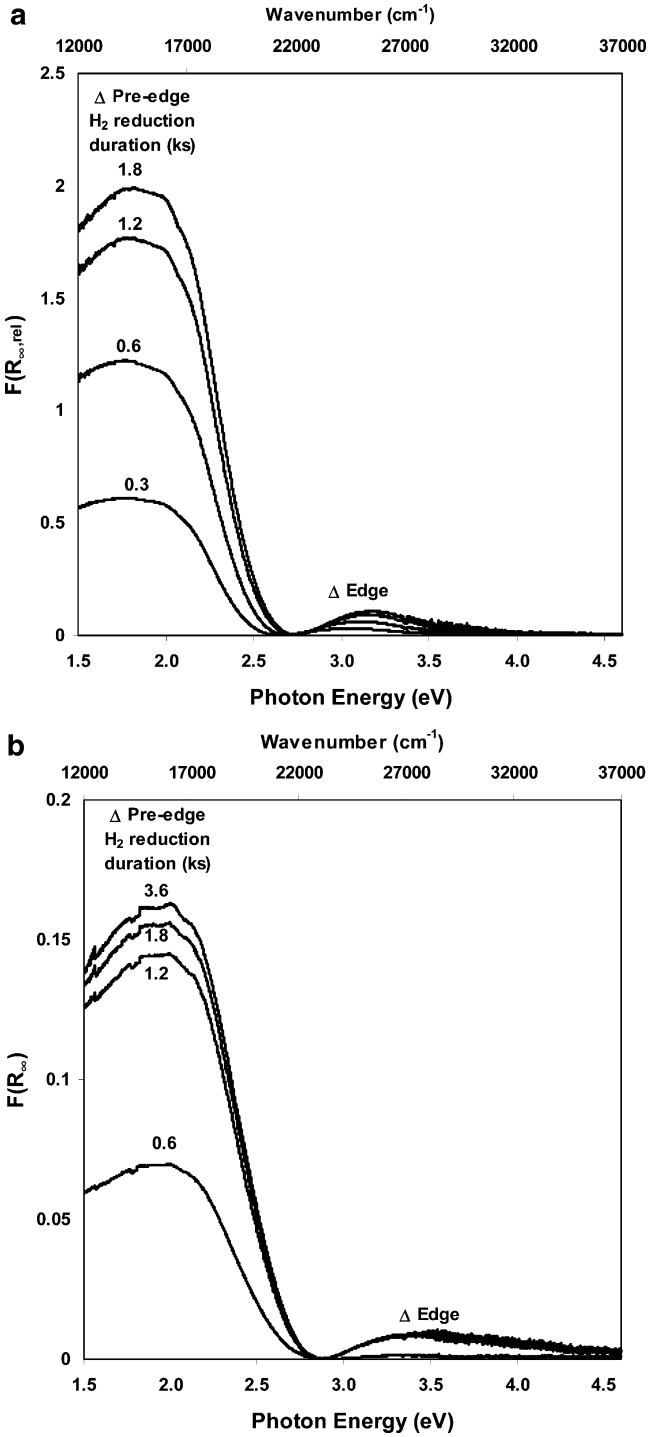

Figure 2. (a) UV−visible spectra of 10 wt % V_2O_5/Al_2O_3 (8.0 V/nm^2) during hydrogen reduction, where the R_∞ reference is the fully oxidized catalyst [101 kPa H_2, 603 K]. (b) UV−visible spectra of 3.5 wt % V_2O_5/Al_2O_3 (2.3 V/nm^2) during hydrogen reduction, where the R_∞ reference is the fully oxidized catalyst [101 kPa H_2, 603 K].

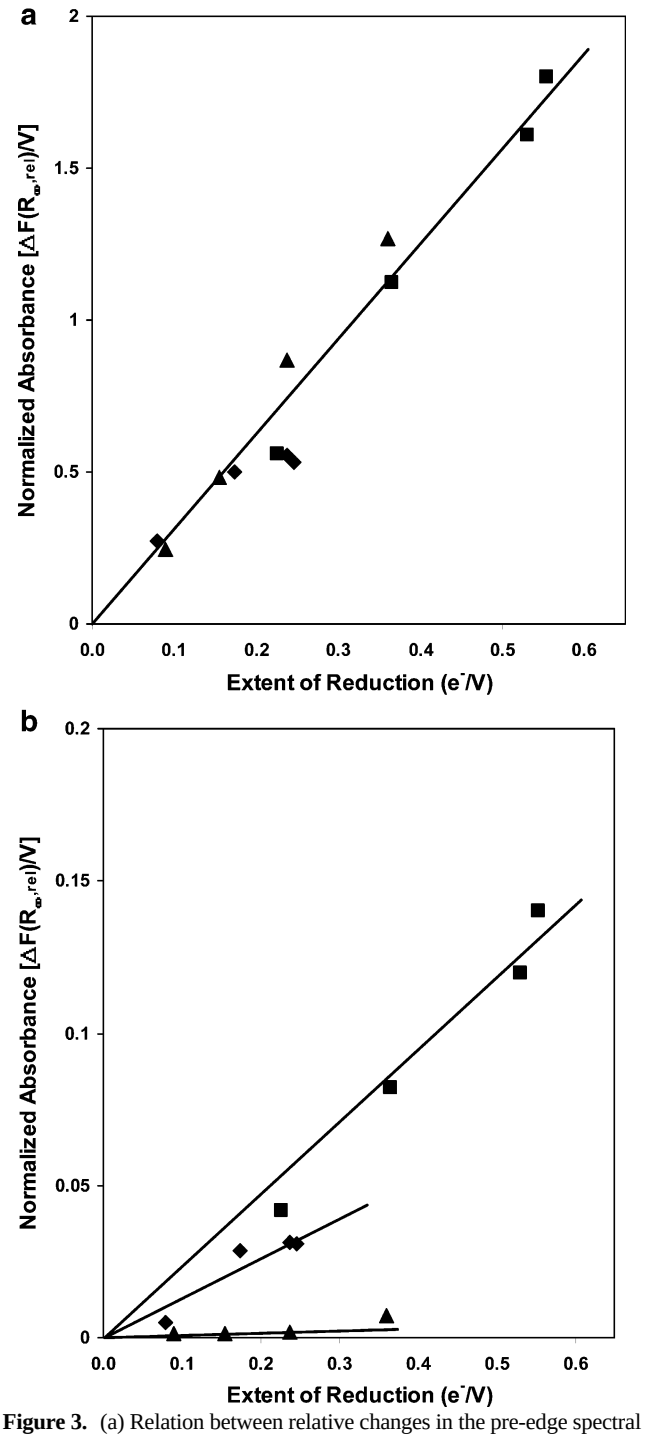

Figure 3. (a) Relation between relative changes in the pre-edge spectral feature during H_2 reduction and the extent of catalyst reduction quantified by subsequent O_2 temperature-programmed oxidation [diamonds: 3.5 wt % V_2O_5/Al_2O_3 (2.3 V/nm^2); squares: 10 wt % V_2O_5/Al_2O_3 (8.0 V/nm^2); triangles: 30 wt % V_2O_5/Al_2O_3 (34 V/nm^2). Hydrogen reduction: 101 kPa H_2 for intervals increasing by 300 s, 603 K; temperature-programmed oxidation: 5 kPa O_2, balance He, room temperature to 773 K, 1.7 K/s ramp rate]. (b) Relation between relative changes in the edge spectral feature during H_2 reduction and the extent of catalyst reduction quantified by subsequent O_2 temperature-programmed oxidation [diamonds: 3.5 wt % V_2O_5/Al_2O_3 (2.3 V/nm^2); squares: 10 wt % V_2O_5/Al_2O_3 (8.0 V/nm^2); triangles: 30 wt % V_2O_5/Al_2O_3 (34 V/nm^2). Hydrogen reduction: 101 kPa H_2 for intervals increasing by 300 s, 603 K; temperature-programmed oxidation: 5 kPa O_2, balance He, room temperature to 773 K, 1.7 K/s ramp rate].

equivalent information and accuracy when the sample absorbance is weak. At higher vanadia surface densities, strong absorption leads to similar edge absorption intensities in fresh and steady-state samples (Figure 2); this leads to inaccurate extents of reduction (±50% at 95% confidence) for the two samples with higher V-content and surface density. Pre-edge calibration data are much more accurate and reproducible (±15% at 95% confidence); they are used here as the preferred method in all subsequent analyses. The measured extents of reduction during steady-state ODH increase and then decrease with increasing vanadium surface density; these trends are discussed in detail below.

TABLE 1: Extent of Vanadium Reduction during Propane ODH Determined from Pre-edge and Edge Absorbance Delta Values[a]

catalyst (wt % V_2O_5 on Al_2O_3)	V surface density (V nm^{-2})	$\Delta e^-/V$ (1.49−1.86 eV)[b]	$\Delta e^-/V$ (2.73−3.53 eV)[c]
3.5	2.3	0.062	0.056
10	8.0	0.30	0.12
30	34	0.084	0.097

[a] 603 K, 14 kPa C_3H_8, 1.7 kPa O_2, balance He. [b] Obtained from pre-edge data (Figure 3a). [c] Obtained from edge data (Figure 3b).

In what follows, we address two critical issues: (1) what fraction of the reduced centers are reactive intermediates relevant to ODH catalysis; and (2) how does the concentration of catalytically relevant reduced centers vary with C_3H_8 and O_2 partial pressures. Figure 4a shows absorption intensities at 1.86 eV for 10 wt % V_2O_5/Al_2O_3 (8.0 V/nm^2) during an extended period (8 h) started after treatment of a fresh sample with 5 kPa O_2 for 773 K for 1 h, cooling to 603 K, and exposure to C_3H_8(1 kPa)−O_2(4 kPa) for 4 h, and then to 4 kPa O_2 at 603 K for 4 h. A fast reduction process occurs during the first ∼120 s after exposure to reactants; this process is followed by a slower reduction process occurring over a 4 h period. Subsequent O_2 exposure leads to a rapid initial oxidation, followed by a slower process, which does not fully restore the initial oxidation state even after 4 h (11% of the steady-state reduced centers remain in their reduced state). Treatment in 5 kPa O_2 at 773 K for several minutes was required to fully restore the spectrum to that of the starting catalyst, suggesting that no significant structural changes, such as sintering or mixed oxide formation, occurred during catalysis. Some of the changes in pre-edge intensity were unrelated to catalytic turnovers and occurred over longer times scales than such turnovers; such catalytically irrelevant reduction events were decoupled from those involved in catalytic cycles by transient experiments, as we discuss in detail below.

These data suggest that some of the reduced centers detected do not undergo redox cycles in the time-scale of catalytic turnovers; these time-scales are <1000 s for the 10 wt % V_2O_5/Al_2O_3 (8.0 V/nm^2) sample (from the inverse of the ODH rate per V-atom in Table 2). Thus, the data in Figure 4a indicate that the formation and oxidation of reduced centers include processes much slower than turnovers and likely to reflect changes in the structure of domains or oxygen removal from internal crystallite regions, which are not relevant to catalytic turnovers.

Reoxidation was also attempted after ODH catalysis by adding 1 kPa H_2O to a stream containing 5 kPa O_2 to probe whether H_2O adsorption−desorption steps (Appendix, eq A4) would enhance vacancy mobility, which is presumably required for O_2 dissociation on proximate vacancies (Appendix, eq A5). Figure 4b shows the absorbance (at 1.86 eV) for 3.5 wt % V_2O_5/Al_2O_3 (2.3 V/nm^2) at 603 K during reoxidation with H_2O (bold line, 1 kPa H_2O, 5.0 kPa O_2) and without H_2O (thin line, 5.0 kPa O_2) after ODH (14 kPa C_3H_8, 1.7 kPa O_2, 603 K, 2 h). Initial reoxidation rates were essentially identical, but H_2O slightly inhibits reoxidation at intermediate times and enhances it slightly at longer times. In any case, the slow reoxidation observed after ODH does not arise from the use of dry O_2 streams, which could have prevented the formation of proximate vacancies required for reoxidation. These slow processes appear to arise instead from oxygen removal from catalytically irrelevant structures, possibly minority V_2O_5 crystallites with low catalytic surface areas.

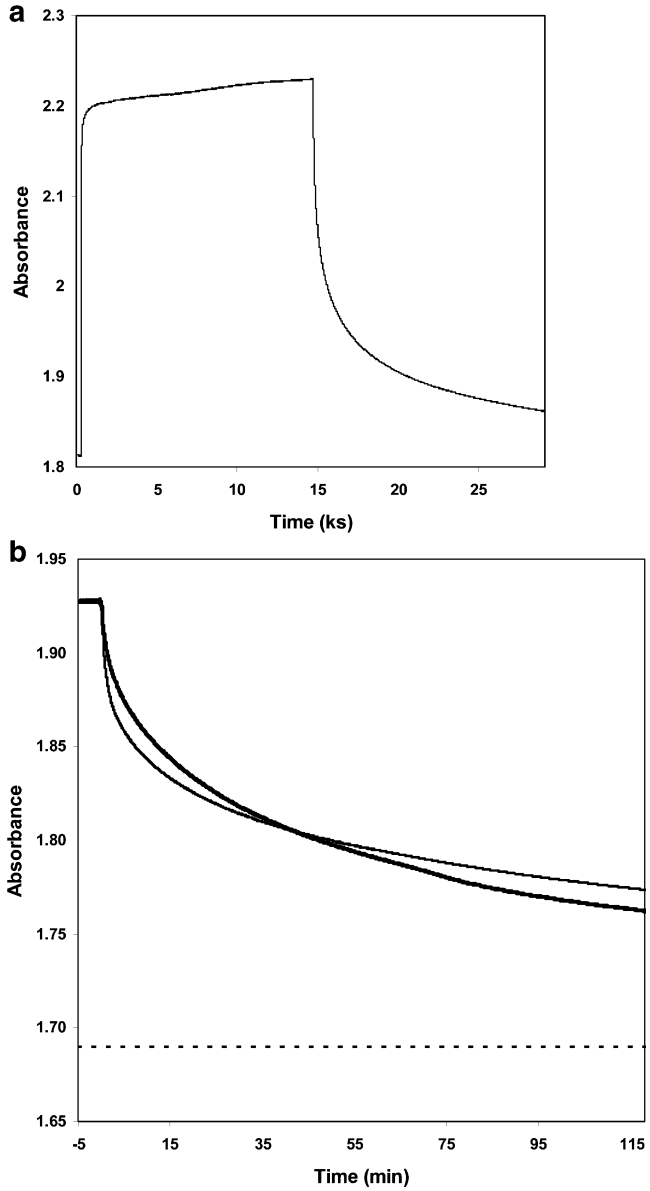

Figure 4. (a) Absorbance response during step change from oxidizing conditions (4.0 kPa O_2, balance Ar) to ODH (1.0 kPa C_3H_8, 4.0 kPa O_2, balance Ar) and back to oxidizing conditions (4.0 kPa O_2, balance Ar) [10 wt % V_2O_5/Al_2O_3 (8.0 V/nm^2), 603 K]. (b) Effect of water addition during reoxidation following propane ODH; thin line: no water added; bold line: 1 kPa water added; dashed line: initial absorbance of stoichiometric oxide [3.5 wt % V_2O_5/Al_2O_3 (2.3 V/nm^2), ODH conditions: 14 kPa C_3H_8, 1.7 kPa O_2, balance Ar, 663 K; reoxidation without H_2O: 5.0 kPa O_2, balance Ar, 603 K, reoxidation with H_2O: 5.0 kPa O_2, 1.0 kPa H_2O, balance Ar, 603 K].

Reduced centers relevant and irrelevant to catalysis must be separately quantified for any in situ measurement to reflect intermediates without contributions from spectator species. The deconvolution of structures of varying catalytic relevance generally requires transient measurements. With this in mind, we carried out UV−visible measurements in which fully oxidized catalysts were exposed to a given reactant composition for 300 s; then, this composition was changed for another 300 s, by varying either the C_3H_8 or O_2 pressure, while keeping the other constant. Figure 5a shows the results of these stepwise changes in C_3H_8 pressure; each reactant cycle is followed by a treatment in 4 kPa O_2 at 603 K for 300 s. The initial transient (0−120 s) is identical to that in Figure 4a. Subsequent transients, during which the C_3H_8 pressure was doubled each time, lead to a rapid increase in absorbance during the first 90 s, which

TABLE 2: Comparison of Total and Catalytically Relevant Extents of Vanadium Reduction during Propane ODH with Measured Propane ODH Rates (7)[a]

catalyst (wt % V_2O_5 on Al_2O_3)	V surface density (V nm^{-2})	$\Delta e^-/V$	$\Delta e^-_{cat}/V$ [b]	C_3H_6 Rate [$*10^{-3}$ mol s^{-1} (g-atom V)$^{-1}$]	$\Delta e^-_{cat}/V_{surface}$ [c]	C_3H_6 Rate [$*10^{-3}$ mol s^{-1} (g-atom $V_{surface}$)$^{-1}$][c]
3.5	2.3	0.062	0.020	0.33	0.020	0.33
10	8.0	0.30	0.12	1.0	0.13	1.1
30	34	0.084	0.035	0.24	0.15	1.1

[a] 603 K, 14 kPa C_3H_8, 1.7 kPa O_2, balance He. [b] Δe^-_{cat} represents catalytically relevant reduced centers. [c] $V_{surface}$ represents surface vanadia (normalized assuming that a maximum of 7.5 V/nm^2 are exposed).

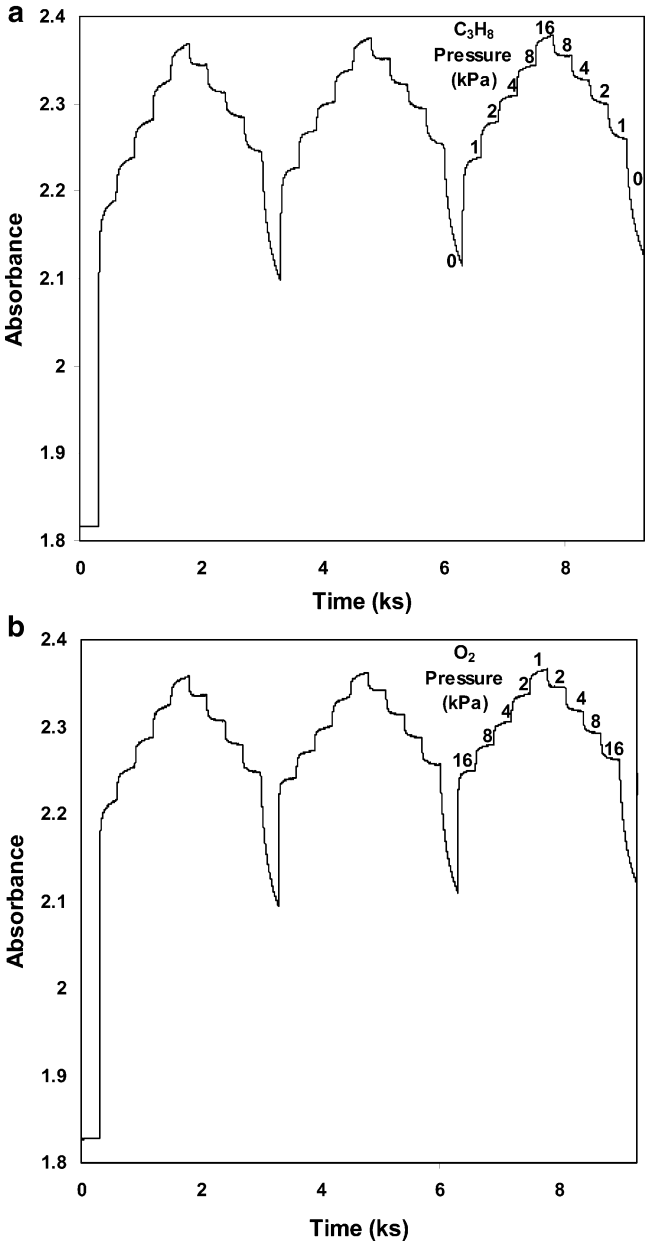

Figure 5. (a) Absorbance response during step changes in C_3H_8 concentration of 300 s duration, starting from the fully oxidized catalyst [10 wt % V_2O_5/Al_2O_3 (8.0 V/nm^2), 603 K, 4.0 kPa O_2, each cycle progresses through 0, 1.0, 2.0, 4.0, 8.0, 16, 8.0, 4.0, 2.0, 1.0 kPa C_3H_8, balance Ar, 603 K]. (b) Absorbance response during step changes in O_2 concentration of 300 s duration, starting from the fully oxidized catalyst [10 wt % V_2O_5/Al_2O_3 (8.0 V/nm^2), 603 K, each cycle begins with 4.0 kPa O_2 and no C_3H_8; upon initiation of ODH with 4.0 kPa C_3H_8, the cycle progresses through 16, 8.0, 4.0, 2.0, 1.0, 2.0, 4.0, 8.0, 16 kPa O_2, balance Ar, 603 K].

becomes much slower with time. The reverse pattern (a fast reoxidation that becomes much slower with time) is observed when C_3H_8 pressure decreases. The rapid changes in absorption observed during a reversible C_3H_8 pressure cycle are identical, indicating that this fraction of the transient change is reversible within time-scales of catalytic turnovers. Also, the absorbance decreases to ~60% of its maximum value during exposure to O_2 for 300 s after ODH reaction for 300 s, and then returns rapidly to its steady-state values after reintroduction of $C_3H_8-O_2$ reactants. The absorbance measured during ODH with 1 kPa of C_3H_8 and 4 kPa of O_2 after a reoxidation cycle gradually increases with increasing number of ODH− reoxidation cycles. This gradual increase occurs over time scales similar to the gradual reduction processes observed over long periods of time in the data shown in Figure 4a. Similar results were obtained with up−down cycles in O_2 partial pressure (Figure 5b). In this case, the experiment was started by switching from a stream containing 4 kPa O_2 to one consisting of 16 kPa O_2 and 4 kPa C_3H_8.

Taken together, these results (Figures 5a and 5b) indicate that the number of catalytically relevant redox centers can be estimated from the rapid initial changes in absorbance that occur after each abrupt change in reactant composition. The rapid initial increase in absorbance upon first switching from O_2 to $C_3H_8-O_2$ streams (Figures 4 and 5) is also irreversible and it is therefore attributed to reduction process that cannot be reversible during ODH catalytic turnovers. Measurements of the catalytically relevant component in these transients can be made more rigorous by examining how the various reduced centers expected to form during ODH depend on C_3H_8 and O_2 concentrations using well-established redox mechanisms.[10,11] Previously reported sequences of elementary steps are expanded here to account for combustion pathways (See Appendix). The pseudo-steady-state approximation for each reactive intermediate led to eqs 4−7, which relate the concentrations of vacancies ([*]), hydroxyl groups ([OH*]), and alkoxide species ([C_3H_7O*]) to the prevalent O_2 and C_3H_8 pressures.

$$[OH^*] = \left\{\lambda_1[C_3H_8] + \lambda_2[H_2O]\left(\frac{[C_3H_8]}{[O_2]}\right)^{1/2}\right\}^{1/2}[O^*] \quad (4)$$

$$[*] = \lambda_3\left(\frac{[C_3H_8]}{[O_2]}\right)^{1/2}[O^*] \quad (5)$$

$$[C_3H_7O^*] = \lambda_4[C_3H_8][O^*]^2 \quad (6)$$

$$[O^*] = [L] - [OH^*] - [*] - [C_3H_7O^*] \quad (7)$$

The λ_i terms contain rate constants and a measure of reaction selectivity, defined as the fraction of the turnovers that lead to propene (vs CO_x). [O*] and [L] are the concentrations of active surface oxygens and total active sites, respectively.

Equations 4−6 show the expected dependence of the number of reduced centers on C_3H_8 (0.5−0.75 power) and O_2 (−0.5 to −0.25 power) pressures and the individual concentrations of vacancies, OH groups, and alkoxides. The trends in reduced

centers with $[O_2]^{-1}$ (Figure 5b) and with $[C_3H_8]$ (Figure 5a) are almost identical, suggesting that the concentration of reduced centers depends only on the C_3H_8/O_2 ratio and not on the individual concentrations of the two reactants at the conditions of low C_3H_8 conversion (<1%) and small water concentration ($<3 \times 10^{-8}$ mol/cm^3) prevalent during these experiments. This functional dependence is consistent only with vacancies as the most abundant reduced centers during ODH (eq 5). The H_2O dependence in the expression for [OH*] (eq 4) leads to an additional dependence on C_3H_8 partial pressure, because the H_2O concentrations are proportional to C_3H_8 pressures (since the first-order dependence of the rate on C_3H_8 leads to invariant conversions with changes in C_3H_8 pressure); thus, [OH*] cannot account for a significant fraction of the prevalent reduced centers.

The proposal that changes in the pre-edge region reflect contributions from active and catalytically irrelevant redox centers was probed by representing the total change in absorbance, $\Delta A(P_n)$, for a given partial pressure P_n of the component whose concentration is perturbed as

$$\Delta A(P_n) = (\Delta A_{\text{noncat}} + \Delta A_1) + \sum_{i=2}^{n} \Delta A_i \qquad (8)$$

The term $(\Delta A_{\text{noncat}} + \Delta A_1)$ represents total absorbance changes shortly after initial contact of fresh samples with reactants. ΔA_{noncat} and ΔA_1 reflect changes in absorbance for catalytically irrelevant and relevant processes, respectively. The ΔA_i terms represent the catalytically relevant changes in absorbance associated with each subsequent step change in reactant pressure (e.g., ΔA_2 for any cycle of increasing absorbance in Figure 5a is the change in absorbance resulting from C_3H_8 increasing from 1 to 2 kPa). The summation term, $\sum_{i=2}^{n} \Delta A_i$, is the total absorbance change of the subsequent variations in partial pressures, excluding the slow upward drift noted in Figure 4a. If we assume vacancies are the predominant active reduced centers responsible for the absorbance changes in Figures 5a and 5b, $\Delta A(P_n)$ would be given by

$$\Delta A(P_n) = \Delta A_{\text{noncat}} + B(P_{C_3H_8}/P_{O_2})_n^{0.5} \qquad (9)$$

which shows the expected sole dependence on C_3H_8/O_2 reactant ratios and which allows estimates of ΔA_{noncat} and B from our experimental data.

Figure 6 shows the catalytically relevant extents of reduction per surface V-atom as a function of C_3H_8/O_2 reactant ratios. A simple geometric model, in which V-atoms in excess of the theoretical monolayer (7.5 V/nm^2)[8,36] become inaccessible, was used to estimate the fraction of V-atoms at surfaces. These extents of reduction are then obtained using the values of $(\Delta A(P_n) - \Delta A_{\text{noncat}})$ from Figures 5a and 5b and calibration curves similar to those in Figure 3a, but accurate for the single energy (1.86 eV) of the data in Figures 5a and 5b. The solid symbols represent data obtained by varying the partial pressure of C_3H_8 (Figure 5a) and the open symbols reflect data obtained by varying O_2 partial pressures (Figure 5b). The two sets of data agree well; they are accurately described by a half-order dependence of the number of catalytically relevant redox centers on the C_3H_8/O_2 reactant ratio, as expected when vacancies are the most abundant reduced centers (eq 5). The data in Figure 6 also show that steady-state extents of reduction for catalytically relevant redox centers are very small (<0.1 $e^-/V_{surface}$), consistent with the assumption, made in deriving eq 9, that [O*] is essentially constant and equal to [L].

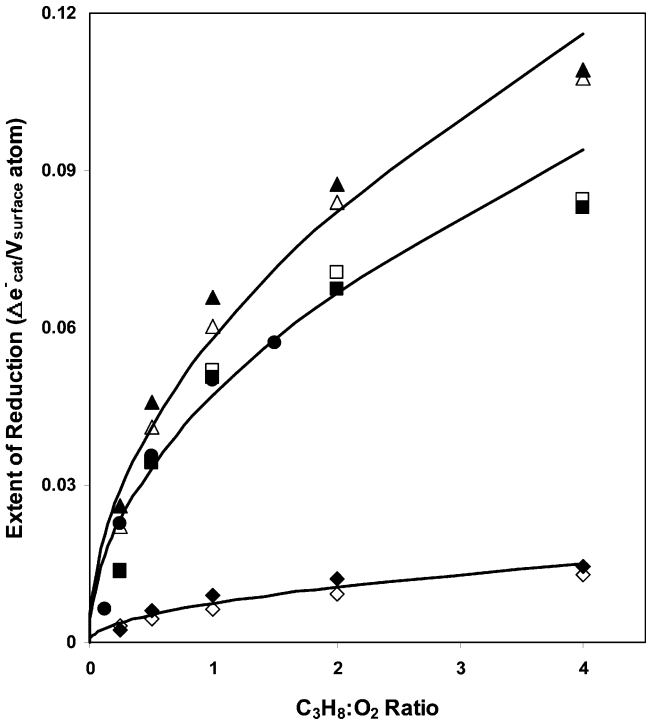

Figure 6. Dependence of the extent of catalytically relevant reduction per surface V-atom on the C_3H_8/O_2 ratio for VO_x/Al_2O_3 catalysts during propane ODH [filled symbols: C_3H_8 dependence (1.0−16 kPa C_3H_8, 4.0 kPa O_2, balance Ar, 603 K); open symbols: O_2 dependence (4.0 kPa C_3H_8, 1.0−16 kPa O_2, balance Ar, 603 K); diamonds: 3.5 wt % V_2O_5/Al_2O_3 (2.3 V/nm^2); squares: 10 wt % V_2O_5/Al_2O_3 (8.0 V/nm^2); triangles: 30 wt % V_2O_5/Al_2O_3 (34 V/nm^2); filled circles are C_3H_8 dependence (8.0 kPa O_2, 1.0−12 kPa O_2, balance Ar, 603 K) for 10 wt % V_2O_5/Al_2O_3 (8.0 V/nm^2)].

The reactant cycles shown in Figures 5a and 5b were started with the same 1:4 C_3H_8/O_2 reactant ratio, but at different individual pressures (1.0 kPa C_3H_8, 4.0 kPa O_2 in Figure 5a and 4.0 kPa C_3H_8, 16 kPa O_2 in Figure 5b). The filled circles in Figure 6 show data for an experiment started at a lower reactant ratio (1:8 C_3H_8/O_2 on 10 wt % V_2O_5/Al_2O_3, 1.0 kPa C_3H_8, 8.0 kPa O_2, 603 K), but otherwise similar to the experiment leading to the data in Figure 5a. The data points for reactant ratios of 1:8 and 1:4 (filled and open squares) coincide, which confirms that extents of reduction for catalytically relevant redox centers (reported in Figure 6) are independent of the initial reactant concentration. ΔA_{noncat} in eqs 8 and 9, however, appears to depend on the initial C_3H_8/O_2 reactant ratio and shows values of 0.18 $\Delta e^-/V_{surface}$ and 0.16 $\Delta e^-/V_{surface}$ for initial reactant ratios of 1:4 and 1:8 C_3H_8/O_2, respectively, on 10 wt % V_2O_5/Al_2O_3 (8.0 V/nm^2).

The number of kinetically-relevant and spectator-reduced centers are compared in Table 2 with the total number of reduced centers (from Table 1); only a fraction of reduced centers are active in catalytic turnovers (32%, 40%, and 42% for 3.5, 10, and 30 wt % V_2O_5/Al_2O_3, respectively). Both the total number of reduced centers and those active in propane ODH turnovers correspond to lower extents of reduction than required for stoichiometric reduction of V^{5+} to V^{4+} (or V^{3+}). These data confirm the conclusions reached from kinetic and isotopic studies[10,11] that lattice oxygen atoms are the most abundant reactive intermediates during propane ODH on VO_x domains, even at relatively high C_3H_8/O_2 reactant ratios (Figure 6, Table 2).

Table 2 also shows propane ODH rates (per V-atom) reported previously[7,8] on the three samples of this study. ODH rates (per V-atom) increase with increasing V-surface density (from 2.3

V/nm^2 to 8.0 V/nm^2), because larger two-dimensional VO_x domains prevalent at higher surface densities undergo redox processes much faster than monovanadate structures present at lower surface densities.[6−9] ODH rates then decrease at higher surface densities, as three-dimensional V_2O_5 crystallites with inaccessible V-atoms become the predominant VO_x species. The maximum ODH rate (per V) at intermediate V surface densities occurs at similar surface densities as the maximum number of reduced centers measured during ODH (Table 2), indicating that exposed VO_x species on larger domains (prevalent at 8.0 V/nm^2) are easier to reduce than isolated monovanadates (at 2.3 V/nm^2). These conclusions are consistent with reduction kinetic studies on VO_x/γ-Al_2O_3 samples with a similar range of VO_x surface densities.[34] VO_x species on larger domains (at 8.0 V/nm^2) also undergo faster redox cycles than isolated VO_x species (at 2.3 V/nm^2).[6−8] This correlation between ODH rates and extents of reduction is consistent with previously reported ODH turnover rates (per V or Mo), which increased with increasing VO_x or MoO_x domain size[6−8,35] (Table 2), and with the sole kinetic relevance of the C−H bond activation step, which requires activated complexes involving significant cation reduction.[10,11] The fraction of V-atoms reduced during steady-state ODH is lower at high surface densities (34 V/nm^2) than at intermediate surface densities (8.0 V/nm^2), because V centers become inaccessible to reactants and cannot undergo redox cycles required for ODH turnovers.

Extents of reduction can be normalized by the number of V-atoms residing at surfaces (Figure 6) estimated in the manner described above. At low surface densities, all V-atoms are essentially exposed; thus, the extent of reduction is unchanged from that estimated on the basis of total V-atoms and shown in Table 2. On the other two samples, normalization by surface V-atoms leads to higher extents of reduction than obtained using the total number of V-atoms, because only a fraction of them are exposed (Table 2; sixth column). The extent of reduction values on a surface V-atom basis increase sharply between 2.3 V/nm^2 and 8.0 V/nm^2 and then reach a nearly constant value for the sample with 34 V/nm^2. ODH rates on the same surface V-atom basis (Table 2, last column) also increase initially with surface density and then reach constant values as the support surface becomes covered with polyvanadate and V_2O_5. The extent of reduction on a surface V basis increases in parallel ODH rates (per surface V-atom), which is expected for a catalytic redox cycle occurring at accessible V centers. The agreement between the trends in extent of reduction and ODH rates corroborates that the reduced centers deemed catalytically relevant are indeed participating in the turnovers that result in propene production.

The extents of reduction reported here for active redox centers on VO_x/Al_2O_3 are much lower than previously reported on VO_x/ZrO_2 at similar propane ODH conditions and VO_x surface densities, from changes in intensity at the UV−visible absorption edge.[17,20] Here, we measure 0.12 e^-_{cat}/V on 8.0 V/nm^2 VO_x/Al_2O_3 at 603 K at 8:1 C_3H_8/O_2, while these previous studies report values of 0.60 e^-/V on 8.0 V/nm^2 VO_x/ZrO_2 at 6:1 C_3H_8/O_2 and lower temperatures (573 K).[17,20] Spectator reduced centers, perhaps even on ZrO_2 supports,[17] may account for these differences, as well as for the much higher CO_x selectivities measured on ZrO_2-supported samples.[8,17]

Conclusions

The number of catalytically relevant reduced centers measured during propane ODH on vanadia catalysts (0.02−0.13 $\Delta e^-_{cat}/V$) is small compared to stoichiometric suboxides of V^{3+} and V^{4+}. Surface oxygen species are the most abundant reactive intermediates during catalysis. The extent of reduction is smaller than previously reported for similar catalysts, apparently due to the presence of spectator reduced species, which do not undergo reversible redox processes in the time scale of catalytic turnovers. The number of catalytically relevant reduced centers depends only on the C_3H_8/O_2 reactant ratio, and not separately on the concentrations of each reactant; this is consistent with vacancies as the most abundant reduced species during catalytic ODH at low propane conversion and water concentrations. The method described here for measuring reduced centers during catalytic oxidation reactions uses pre-edge features in the UV−visible spectrum. It is more sensitive and accurate than previously reported techniques based on near-edge changes in X-ray absorption and UV−visible spectra. Mild H_2 reduction followed by quantitative reoxidation by O_2 allows a rigorous and accurate calibration of the number of reduced centers present at the low extents of reduction prevalent during ODH reactions. The number of catalytically relevant reduced centers during ODH increases in parallel with ODH rates (per surface V-atom) as the size of vanadia domains increases with increasing surface density. These findings are consistent with the redox nature of the catalytic ODH sequence, with the sole kinetic relevance of C−H bond activation reduction steps, and with the greater reducibility of larger vanadia domains.

Acknowledgment. This work was supported by the Director, Office of Basic Energy Sciences, Chemical Sciences Division of the U.S. Department of Energy under Contract DE-AC03-76SF00098.

Appendix

The proposed mechanism for propane oxidative dehydrogenation and combustion reactions is shown in the following scheme:

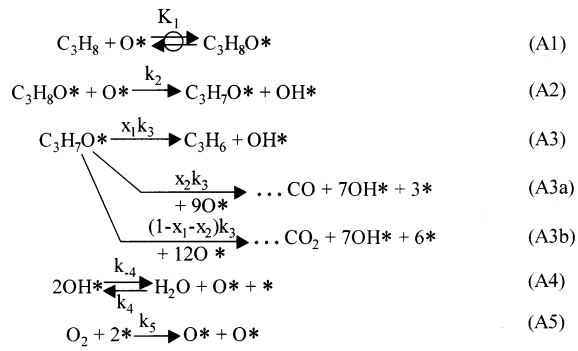

where x_1 and x_2 are the carbon-normalized selectivities to C_3H_6 and CO, respectively.

The nonlinear differential equations describing the time-dependent response of the surface species are

$$\frac{d[O^*]}{dt} = -2k_2K_1[C_3H_8]\frac{[O^*]^2}{L} - 3(4 - 4x_1 - x_2)k_3[C_3H_7O^*] + k_{-4}\frac{[OH^*]^2}{[L]} - k_4[H_2O]\frac{[O^*][^*]}{[L]} + 2k_5[O_2]\frac{[^*]^2}{[L]} \quad (A6)$$

$$\frac{d[OH^*]}{dt} = k_2K_1[C_3H_8]\frac{[O^*]^2}{[L]} + (7 - 6x_1)k_3[C_3H_7O^*] - 2k_{-4}\frac{[OH^*]^2}{[L]} + 2k4[H_2O]\frac{[O^*][^*]}{[L]} \quad (A7)$$

$$\frac{d[C_3H_7O^*]}{dt} = k_2K_1[C_3H_8]\frac{[O^*]^2}{[L]} - k_3[C_3H_7O^*] \quad (A8)$$

$$\frac{d[^*]}{dt} = 3(2 - 2x_1 - x_2)k_3[C_3H_7O^*] + k_{-4}\frac{[OH^*]^2}{[L]} - k_4[H_2O]\frac{[O^*][^*]}{[L]} - 2k_5[O_2]\frac{[^*]}{[L]} \quad (A9)$$

The pseudo-steady-state solutions for the surface intermediates are

$$\frac{[O^*]}{[L]} = 1 - \frac{[OH^*]}{[L]} - \frac{[^*]}{[L]} - \frac{[C_3H_7O^*]}{[L]} \quad (A10)$$

$$[OH^*] = \{(8 - 6x_1)(k_2K_1/2k_{-4})[C_3H_8] + (k_2/2k_{-4})[H_2O][2(10 - 9x - 3x_2)(k_2K_1/k_5) \times ([C_3H_8]/[O_2])]^{1/2}\}^{1/2}[O^*] \quad (A11)$$

$$[^*] = [2(10 - 9x_1 - 3x_2)(k_2K_1/4k_5)([C_3H_8]/[O_2])]^{1/2}[O^*] \quad (A12)$$

$$[C_3H_7O^*] = (k_2K_1/k_3)[C_3H_8][O^*]^2/[L] \quad (A13)$$

References and Notes

(1) Kung, H. H. *Adv. Catal.* **1994**, *40*, 1.
(2) Mamedov, E. A.; Cortés Corberán, V. *Appl. Catal. A* **1995**, *127*, 1.
(3) Albonetti, S.; Cavani, F.; Trifirò, F. *Catal. Rev.—Sci. Eng.* **1996**, *38*, 413.
(4) Blasco, T.; López Nieto, J. M. *Appl. Catal. A* **1997**, *157*, 117.
(5) Bañares, M. A. *Catal. Today* **1999**, *51*, 319.
(6) Chen, K. D.; Khodakov, A.; Yang, J.; Bell, A. T.; Iglesia, E. *J. Catal.* **1999**, *186*, 325.
(7) Argyle, M. D.; Chen, K. D.; Bell, A. T.; Iglesia, E. *J. Catal.* **2002**, *208*, 139.
(8) Khodakov, A.; Olthof, B.; Bell, A. T.; Iglesia, E. *J. Catal.* **1999**, *181*, 205.
(9) Olthof, B.; Khodakov, A.; Bell, A. T.; Iglesia, E. *J. Phys. Chem. B* **2000**, *104*, 1516.
(10) Chen, K. D.; Bell, A. T.; Iglesia, E. *J. Phys. Chem. B* **2000**, *104*, 1292.
(11) Chen, K. D.; Iglesia, E.; Bell, A. T. *J. Catal.* **2001**, *192*, 197.
(12) Coulston, G. W.; Bare, S. R.; Kung, H.; Birkeland, K.; Bethke, G. K.; Harlow, R.; Herron, N.; Lee, P. L. *Science* **1997**, *275*, 191.
(13) Eon, J. G.; Olier, R.; Volta, J. C. *J. Catal.* **1994**, *145*, 318.
(14) Vuurman, M. A.; Wachs, I. E. *J. Phys. Chem.* **1992**, *96*, 5008.
(15) Weber, R. S. *J. Catal.* **1995**, *151*, 470.
(16) Brus, L. E. *J. Chem. Phys.* **1984**, *80*, 4403.
(17) Gao, X.; Jehng, J. M.; Wachs, I. E. *J. Catal.* **2002**, *209*, 43.
(18) Puurunen, R. L.; Beheydt, B. G.; Weckhuysen, B. M. *J. Catal.* **2001**, *204*, 253.
(19) Gao, X.; Bare, S. R.; Fierro, J. L. G.; Wachs, I. E. *J. Phys. Chem. B* **1999**, *103*, 618.
(20) Gao, X.; Banares, M. A.; Wachs, I. E. *J. Catal.* **1999**, *188*, 325.
(21) Gao, X.; Bare, S. R.; Weckhuysen, B. M.; Wachs, I. E. *J. Phys. Chem. B* **1998**, *102*, 10842.
(22) Wei, D.; Wang, H.; Feng, X.; Chueh, W.; Ravikovitch, P.; Lyubovsky, M.; Li, C.; Takeguchi, T.; Haller, G. L. *J. Phys. Chem. B* **1999**, *103*, 2113.
(23) Grubert, G.; Rathousky, J.; Schulz-Ekloff, G.; Wark, M.; Zukal, A. *Microporous Mesoporous Mater.* **1998**, *22*, 225.
(24) Melsheimer, J.; Mahmoud, S. S.; Mestl, G.; Schlogl, R. *Catal. Lett.* **1999**, *60*, 103.
(25) Weckhuysen, B. M. *Chem. Commun.* **2002**, 97.
(26) Weckhuysen, B. M.; Verberckmoes, A. A.; Debaere, J.; Ooms, K.; Langhans, I.; Schoonheydt, R. A. *J. Catal.* **2000**, *151*, 115.
(27) Weckhuysen, B. M.; Schoonheydt, R. A. *Catal. Today* **1999**, *49*, 441.
(28) Brückner, A. *Chem. Commun.* **2001**, 2122.
(29) Argyle, M. D.; Chen, K. D.; Resini, C.; Krebs, C.; Bell, A. T.; Iglesia, E. *Chem. Commun.* **2003**, 2082.
(30) Kubelka, P.; Munk, F. *Z. Tech. Phys.* **1931**, *12*, 593.
(31) Kortüm, G. *Reflectance Spectroscopy*; Springer-Verlag: Berlin, 1969.
(32) Delgass, W. N.; Haller, G. L.; Kellerman, R.; Lunsford, J. H. *Spectroscopy in Heterogeneous Catalysis*; Academic Press: New York, 1979.
(33) Cotton, F. A.; Wilkinson, G.; Gaus, P. L. *Basic Inorganic Chemistry*, 3rd ed.; Wiley: New York, 1995.
(34) Kanervo, J. M.; Harlin, M. E.; Krause, A. O. I.; Bañares, M. A. *Catal. Today* **2003**, *78*, 171.
(35) Chen, K. D.; Bell, A. T.; Iglesia, E. *J. Catal.* **2002**, *209*, 35.
(36) Centi, G. *Appl. Catal. A* **1996**, *147*, 267.